ARTICLES

A genome-wide transgenic RNAi library for conditional gene inactivation in *Drosophila*

Georg Dietzl[1,2], Doris Chen[1], Frank Schnorrer[2], Kuan-Chung Su[1], Yulia Barinova[1], Michaela Fellner[1,2], Beate Gasser[1], Kaolin Kinsey[1,2], Silvia Oppel[1,2], Susanne Scheiblauer[1], Africa Couto[2], Vincent Marra[1], Krystyna Keleman[1,2] & Barry J. Dickson[1,2]

Forward genetic screens in model organisms have provided important insights into numerous aspects of development, physiology and pathology. With the availability of complete genome sequences and the introduction of RNA-mediated gene interference (RNAi), systematic reverse genetic screens are now also possible. Until now, such genome-wide RNAi screens have mostly been restricted to cultured cells and ubiquitous gene inactivation in *Caenorhabditis elegans*. This powerful approach has not yet been applied in a tissue-specific manner. Here we report the generation and validation of a genome-wide library of *Drosophila melanogaster* RNAi transgenes, enabling the conditional inactivation of gene function in specific tissues of the intact organism. Our RNAi transgenes consist of short gene fragments cloned as inverted repeats and expressed using the binary GAL4/UAS system. We generated 22,270 transgenic lines, covering 88% of the predicted protein-coding genes in the *Drosophila* genome. Molecular and phenotypic assays indicate that the majority of these transgenes are functional. Our transgenic RNAi library thus opens up the prospect of systematically analysing gene functions in any tissue and at any stage of the *Drosophila* lifespan.

Geneticists have traditionally sought to gain insight into complex biological processes through forward genetic screens. Mutations are generated at random, phenotypes of interest are scored, and the mutated gene is subsequently identified. This approach has been remarkably successful, but is limited by inherent biases in mutagenesis techniques, the large numbers of mutants that must be analysed, and the considerable effort that is still required to identify the relevant genetic lesions. Moreover, most genes have multiple functions, and a gene's function in one tissue can preclude its recovery in screens focused on functions in other tissues. This is particularly true for genes that are essential in the early development of the organism.

The inhibition of gene function by RNAi[1], coupled with the availability of annotated genome sequences, now enables systematic surveys of gene function by reverse genetics. One by one, the function of almost every predicted gene can be disrupted and the phenotypic consequences observed. Any phenotype is immediately linked to a specific DNA sequence. This method has been successfully used in genome-wide screens by applying double-stranded RNAs to *Drosophila melanogaster*[2] or mammalian[3,4] cells in culture. These cell-based assay systems enable detailed studies of many basic cellular processes, but not the complex biology of whole organisms. Large-scale RNAi-based surveys of gene function *in vivo* have thus far been limited to the nematode *Caenorhabditis elegans*[5–8] and the planarian *Schmidtea mediterranea*[9]. However, in these organisms, RNAi is systemic[1,10], and so gene interference cannot easily be restricted to a specific cell type.

In *Drosophila*, RNAi is cell autonomous[11,12] and can be triggered by the expression of a long double-stranded 'hairpin' RNA from a transgene containing a gene fragment cloned as an inverted repeat[13–16]. Using the binary GAL4/UAS expression system[17], such RNAi transgenes can be used flexibly to target gene inactivation to potentially any desired cell type at any stage of the animal's lifespan. If a genome-wide library of transgenic RNAi strains were available, it would thus be possible to conduct systematic RNAi screens targeted to specific cell types in the intact animal. Here we report the generation and validation of such a library.

A genome-wide transgenic RNAi library

We first constructed a library of UAS-driven inverted repeat (*UAS-IR*) transgenes by cloning short gene fragments as inverted repeats into a modified pUAST vector[17], pMF3 (Fig. 1a). PCR primers were designed to amplify fragments from every predicted protein-coding gene in Release 4.3 of the *Drosophila* genome sequence. Where possible, we targeted a single coding exon common to all predicted transcripts of a given gene, and used genomic DNA as a PCR template (77.8%). For some genes it was necessary to include multiple exons, or 5′ or 3′ UTRs, in which case mixed-stage complementary DNA was used as a template (22.2%). We successfully cloned 15,072 *UAS-IR* constructs, representing 13,327 different genes (97.0% of predicted protein-coding genes; Supplementary Table 1). The size of the gene fragment in each inverted repeat varies from 109 to 415 base pairs (bp), with a mean of 323 bp (Fig. 1b).

The inverted repeat sequence for each construct was predicted using e-PCR[18] with low stringency criteria. In most cases (98.4%), a single product was predicted; only 380 primers pairs were predicted to amplify multiple products. We directly sequenced both halves of the inverted repeat for all 380 ambiguous primer pairs, as well as 192 of the unambiguous pairs. This confirmed that the intended product had been cloned for all of the unambiguous pairs, and all but 20 of the ambiguous pairs. These 20 anomalous clones consisted of different PCR products cloned head-to-head, and were discarded. Amongst the remaining 552 sequence-verified RNAi constructs, 8 had a deletion in one or both halves of the inverted repeat (ranging in size from 18 to 100 bp); the remaining 544 corresponded exactly to the

[1]Institute of Molecular Biotechnology of the Austrian Academy of Sciences (IMBA), Dr. Bohr-Gasse 3-5, A-1030 Vienna, Austria. [2]Research Institute of Molecular Pathology (IMP) Dr. Bohr-Gasse 7, A-1030 Vienna, Austria.

predicted sequence. We thus estimate that ~98.5% of the RNAi constructs contain the complete intended inverted repeat, whereas ~1.5% contain inverted repeats that are slightly smaller than intended but still likely to trigger RNAi.

The validated *UAS-IR* constructs were then used to generate a library of transgenic RNAi strains by germline transformation[19] of an isogenic w^{1118} host[20]. Each insertion was verified by amplification of the appropriate-sized product from genomic DNA by PCR with a vector- and gene-specific primer pair (Fig. 1a). We mapped each verified insertion to a specific chromosome and established homozygous or balanced stocks, retaining the isogenic w^{1118} background throughout. In all, we obtained 22,270 transgenic RNAi lines, representing 13,251 RNAi constructs and 12,088 genes (88.0% of predicted protein-coding genes; Supplementary Table 2).

Target predictions

To assess the targeting potential of each RNAi construct, we conceptually 'diced' the predicted hairpin RNA into all possible 19-mers because RNAi-mediated degradation of a target messenger RNA generally requires a perfect match of at least 19 nucleotides[21]. We then interrogated the predicted *Drosophila* transcriptome for all perfect matches to these 19-mers, in both the sense and antisense orientations. By design, all 19-mers from a *UAS-IR* construct match its primary target gene. In general, it will also be both desirable and unavoidable to additionally target any other gene with very high sequence similarity. Accordingly, we defined an on-target gene as any gene hit by at least 80% of a construct's 19-mers. Any gene hit by fewer 19-mers, but at least one, is considered a potential off-target gene. By these criteria, 14,612 constructs (96.9%) have a single on-target gene. Less than half of the *UAS-IR* constructs have off-target genes (5,889; 39.1%), and most of these are hit by <1% of the construct's 19-mers (Fig. 1c).

As a further measure of targeting specificity, we defined a specificity score, s_{19}, as the number of all on-target 19-mer matches divided by the total number of matches (that is $s_{19} = \Sigma$ on-target matches / (Σ on-target matches + Σ off-target matches)). Thus, $s_{19} = 1$ for a *UAS-IR* construct with no off-target hits, and $s_{19} = 0$ for a (hypothetical) construct with only off-target hits. In our *UAS-IR* collection, $s_{19} \geq 0.80$ for 14,365 constructs (95.3%) (Fig. 1d). Our experience until now suggests that this is likely to be a fairly conservative threshold, as we have observed specific effects even with constructs having a much lower s_{19} score. Another potential source of off-target effects are CAN repeats, with double stranded RNAs containing more than 13 consecutive CANs prone to cause non-specific effects[22]. Only 119 (0.8%) of our RNAi constructs include more than 10 consecutive CANs (Supplementary Table 1).

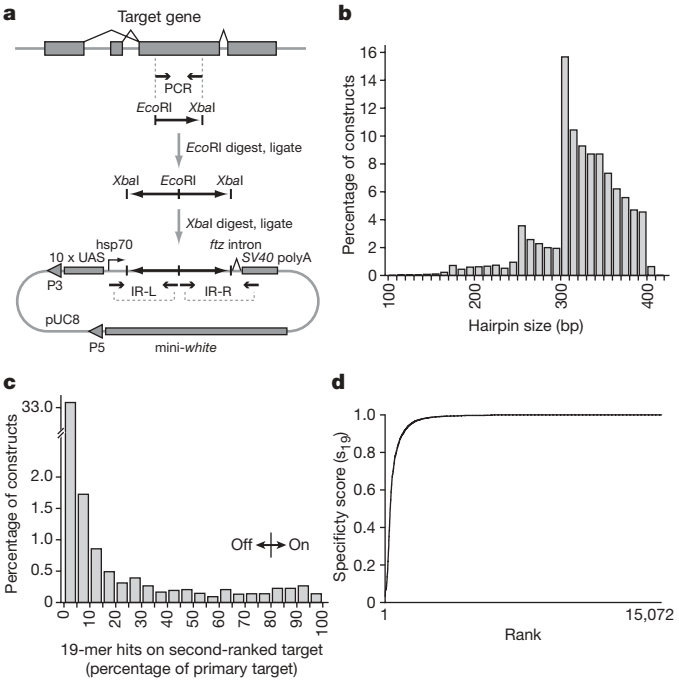

Figure 1 | A genome-wide transgenic RNAi library. a, Strategy used to generate *UAS-IR* constructs. Restriction sites in the original PCR primers were used to digest and ligate PCR products, followed by ligation of the inverted repeat into the pMF3 vector. pMF3 contains 10 GAL4-responsive UAS elements, the basal *hsp70* promoter, the 150 bp second intron of *ftz* and the SV40 polyadenylation signal. Most, but not all, inverted repeats were cloned in the antisense-sense orientation using *Eco*RI and *Xba*I as indicated. IR-L and IR-R indicate the primer pairs used to amplify the left or right halves, respectively, of the inverted repeat. P3 and P5 indicate P-element ends. **b**, Inverted repeat size distribution in 10 bp bins. **c**, Distribution of second-ranked targets, binned according to number of 19-mer matches (primary target = 100%). Any gene hit by less than 80% of 19-mers was considered an off-target hit. For 9,134 constructs (60.6%), the only hit was the primary target. **d**, s_{19} specificity scores for all 15,072 constructs, ranked by specificity.

Targeting *in vivo*

To test the efficiency of RNA knock-down, we selected a set of 64 *UAS-IR* lines (see Methods) and prepared total RNA from *Act5C-GAL4/UAS-IR* animals and *Act5C-GAL4/+* controls. RNA levels for the target gene in the knock-down and control adults were measured using quantitative PCR with reverse transcription (RT–PCR). RNA levels were reduced to less than 25% of the corresponding controls in 25 of the 64 lines (Fig. 2a and Supplementary Table 3). This is likely to underestimate the typical RNA knock-down effect, because we were restricted for this test set to lines that are viable in combination with *Act5C-GAL4*. We presume that RNA levels are generally even more strongly reduced in those lines that are lethal with *Act5C-GAL4* (~32%, see below). It is also unlikely that *Act5C-GAL4* is highly expressed in all cells at all times, and so the efficiency of knock-down in individual cells may well exceed this whole-animal estimate.

As a functional test of RNA knock-down, we selected a positive control set of 432 genes for which classical genetic methods have documented a lethal or visible mutant phenotype. For these genes, we had 658 transgenic RNAi lines in our collection (selecting only those with ≤5 CAN repeats and $s_{19} \geq 0.80$). We also selected 499 genes at random, for which we had 723 RNAi lines. Each of these lines was crossed in duplicate to *Act5C-GAL4* and the progeny screened for lethality or any of 159 distinct defects in adult morphology (Supplementary Table 4). For the positive control set, we observed a phenotype with at least one line for 282 genes (65.3%), and in total for 372 lines (60.1%) (Fig. 2b). Examples of morphological phenotypes are shown in Fig. 2c, along with the corresponding loss-of-function mutants as controls. For the random set, 186 genes (37.3%) covered by 225 lines (31.9%) produced a phenotypic defect (Fig. 2b).

From the positive control set, we estimate the overall false-negative rate for our library at 39.9% of lines and 34.7% of genes. These false-negative rates can almost certainly be reduced by more detailed phenotypic analyses, the use of different *GAL4* driver lines, and methods to enhance RNAi potency, as shown below. Assessing false-positive rates is much more problematic because it is difficult to reliably identify negative control genes. We could however define a negative control set of 48 genes for which classical genetics has provided strong evidence that null mutations result in either no phenotype or a specific visible phenotype. We tested the 63 lines we had for these genes with *Act5C-GAL4*, scoring them for lethality and the same set of 159 morphological defects as the positive controls and randomly selected lines. An unexpected phenotype was observed for only one line (Fig. 2b). We thus estimate that the false-positive rate is likely to be below 2% of lines. It should, however, be noted that we selected lines with ≤5 CAN repeats and $s_{19} \geq 0.80$ for all of these analyses. We have not systematically tested the small fraction of *UAS-IR* constructs

predicted to have a high risk of off-targeting, but anticipate that false-positive rates will be significantly higher for these constructs[21,22].

Tissue-specific RNAi

The availability of a diverse set of *GAL4* drivers[23] allows the transgenic RNAi library to be used to target gene inactivation to almost any desired cell type. Unlike conventional mosaic strategies using classical mutations, transgenic RNAi is not restricted to cells that are clonally related. To test the feasibility of using our library in such experiments, we selected 50 lines that were lethal in combination with the *Act5C-GAL4* driver and crossed each of them separately to *GAL4* drivers that target gene interference to the wing (*MS1096-GAL4*; an enhancer trap in the *Bx* gene), eye (*ey-GAL4, GMR-GAL4*), or notum (*pnr-GAL4*). Approximately 30% of the lines were also lethal with each of these drivers, most probably owing to a vital gene function in the target tissue or in other cells in which the driver is additionally expressed. However, the majority of lines were viable with the tissue-specific drivers, and 25–35% resulted in specific morphological defects (Fig. 3a, b). Different sets of lines produced phenotypes with different *GAL4* drivers, such that 80% of the lines produced a lethal or visible phenotype with at least one driver. These data illustrate the power of transgenic RNAi to uncover tissue-specific functions of essential genes.

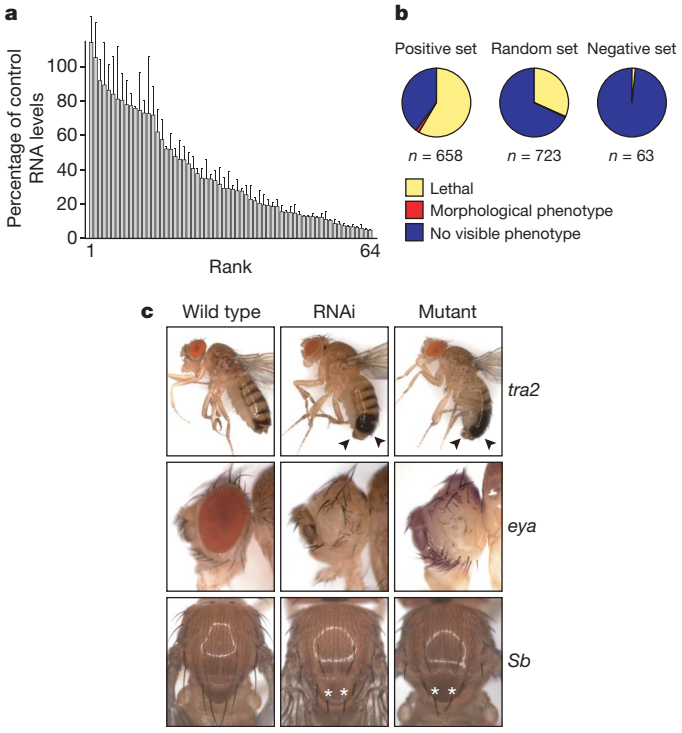

Figure 2 | Efficient and specific gene interference with ubiquitous RNAi. **a**, Efficiency of RNAi-mediated knock-down, as assessed using quantitative RT–PCR on RNA prepared from viable *Act5C-GAL4/UAS-IR* adults and controls. Sixty-four test genes are ranked according to degree of knock down. Data are mean ± s.e.m. ($n = 2$). **b**, Percentages of positive-control, random and negative-control lines producing lethality or an adult morphology phenotype in combination with *Act5C-GAL4*. The only unexpected phenotype in the negative-control set was the lethality of RNAi against *Dredd*. **c**, Examples of morphological phenotypes resulting from ubiquitous RNAi (middle) compared to a classical loss-of-function mutation (right) and wild type (left). Transformer 2 (*tra2*) RNAi and mutant females anatomically resemble males, including male genitalia and abdominal pigmentation (arrowheads). The eyes are greatly reduced or absent in eyes absent *(eya)* RNAi and mutant males, and Stubble (*Sb*) males have short, stubby bristles on the notum (asterisks indicate the shortened scutellar bristles).

Dicer-2 enhances RNAi potency

For our positive-control set, the RNAi phenotypes sometimes corresponded to the null phenotypes reported for classical mutations, but more often resembled a hypomorphic phenotype. This is consistent with the partial reduction in target mRNA levels generally observed for these lines (Fig. 2a). We wondered whether overexpression of components of the RNAi machinery might enhance such phenotypes. In preliminary experiments in which we overexpressed several different factors involved in RNAi (dicer-1, ref. 24; dicer-2, ref. 25; argonaute-1, ref. 26; argonaute-2, ref. 27; *R2D2*, ref. 28; and *tudor-SN*, ref. 29), we found that only dicer-2 (*Dcr-2*) consistently enhanced the transgenic RNAi effect.

When we retested the same set of 50 lines with both the eye and notum drivers, this time co-expressing *UAS-Dcr-2*, we observed an enhanced RNAi effect with 54% and 43% of the lines, respectively (Fig. 3a, b). We suspected that *UAS-Dcr-2* might also increase off-targeting effects, and so also tested 53 lines (41 genes) from the negative control set (Fig. 2b). In both the eye and notum, the false-positive rate increased by 6% in the presence of *UAS-Dcr-2*. We conclude that co-expression of *UAS-Dcr-2* is likely to be a useful approach to enhance transgenic RNAi effects, but caution that it may also enhance off-targeting effects. We recommend that reliability of *Dcr-2* overexpression be tested carefully for each driver and assay.

Targeting neurons and muscles with RNAi

Conditional RNAi transgenes also allow genes to be inactivated specifically in internal tissues that are difficult or impossible to target by classical genetics. Entire neuronal or muscle networks are prime examples. The complexity of these tissues, and in the case of muscles also their multinuclear structure, renders them essentially inaccessible to conventional mosaic strategies involving mitotic recombination. To test the feasibility of RNAi screens targeted to neurons or muscles, we compiled two complementary sets of positive-control genes: 32 genes known or predicted to act in neurons and 27 genes required in muscles (but neither set exclusive to the respective tissue). Our library contains 49 and 42 transgenic RNAi lines, respectively, for these two gene sets. We also selected an additional 129 lines at random, each representing a different gene (Fig. 4a). The RNAi lines in each of these three sets were crossed in duplicate to either the pan-neuronal driver *elav-GAL4* (ref. 30) or the pan-muscle driver *mef2-GAL4* (ref. 31). On the basis of preliminary experiments, we used *UAS-Dcr-2* with *elav-GAL4* but not with *mef2-GAL4*. Progeny were scored for viability and eight simple behavioural defects (Fig. 4b, c).

A lethal or behavioural phenotype was observed in 82% of the neuronal positive-control set tested with *elav-GAL4* (Fig. 4a, b), and 93% of the muscle positive-control set tested with *mef2-GAL4* (Fig. 4a, c). These results demonstrate that transgenic RNAi is potent in both neurons and muscles, and further indicate that, with the appropriate drivers and assay conditions, false-negative rates can indeed be significantly lower than we estimated from the *Act5C-GAL4* data (Fig. 2b). Hit rates amongst the randomly selected lines were 7% with *elav-GAL4* and 14% with *mef2-GAL4*, with 5% positive with both drivers (Fig. 4a).

Conclusions

Our work provides the resources and proof-of-principle for genome-wide tissue-specific RNAi screens in *Drosophila*. All of these RNAi lines are publicly available (http://www.vdrc.at). We estimate that over 60% of these lines trigger potent and specific gene interference, and as many as 90% may be functional in combination with the appropriate drivers, assays, and RNAi-enhancing tools such as *UAS-Dcr-2*. As for RNAi in general, our library is subject to the variable efficiency of gene knock-down and the inherent risk of off-targeting effects. Additionally, because our transgenes are inserted at random sites, some false negatives may be caused by poor transgene expression and some false positives by the misregulation of flanking

endogenous genes. Ultimately, these minor limitations might be overcome by the generation of a second independent library of RNAi transgenes (http://www.shigen.nig.ac.jp/fly/nigfly).

Our transgenic RNAi library offers a powerful alternative to classical forward genetic screens. Although mutagenesis screens will continue to be useful, particularly for early embryonic development, transgenic RNAi screens should be especially suitable for later stages and whenever tissue-specific gene disruption is required. Indeed, transgenic RNAi offers the only practical way to genetically screen certain cell types, such as neurons or muscle. Vast collections of *GAL4* driver lines are already available to target RNAi to specific cells[23], and inducible GAL4 systems can be used to further restrict RNAi to a selected stage of the fly's lifespan[32–34]. Combined with these versatile GAL4 expression systems, our transgenic RNAi library opens up almost limitless possibilities for exploring the genetics of *Drosophila* development, physiology and pathology.

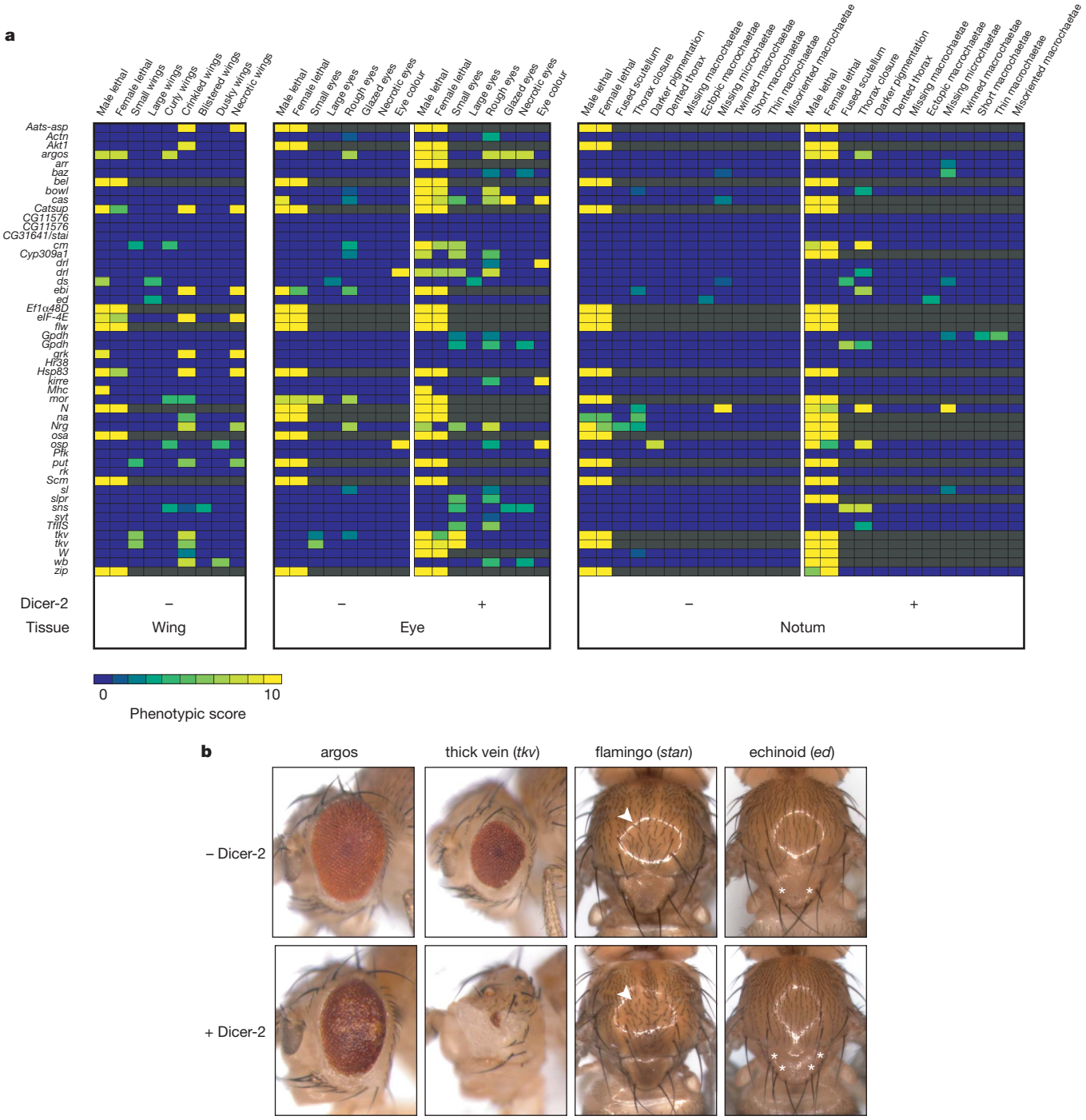

Figure 3 | Tissue-specific RNAi and the enhancing effect of Dicer-2. **a**, Phenotypic data for 50 RNAi lines, representing 46 genes (left), in combination with either *MS1096-GAL4* (wing), *ey-GAL4* and *GMR-GAL4* (eye), or *pnr-GAL4* (notum). For the eye and notum, assays were performed with (+) or without (−) an additional *UAS-Dcr-2* transgene. All phenotypes were scored on a subjective 0–10 scale, with 0 representing no observable defect and 10 the most severe. Phenotypic scores are colour-coded, with grey indicating no data due to lethality. All scores are the average of two independent replicates. **b**, Examples of RNAi phenotypes in the eye and notum. Wild-type controls are shown in Fig. 2c. RNAi against *argos* results in eye roughening, and RNAi against *tkv* leads to eyes that are both rough and reduced in size. RNAi against flamingo (*stan*) leads to a defect in planar cell polarity, evident in the misorientation of microchaetae (arrowheads), whereas RNAi against *ed* results in the formation of ectopic macrochaetae (asterisks). All of the defects shown here are enhanced by co-expression of *UAS-Dcr-2* (bottom row).

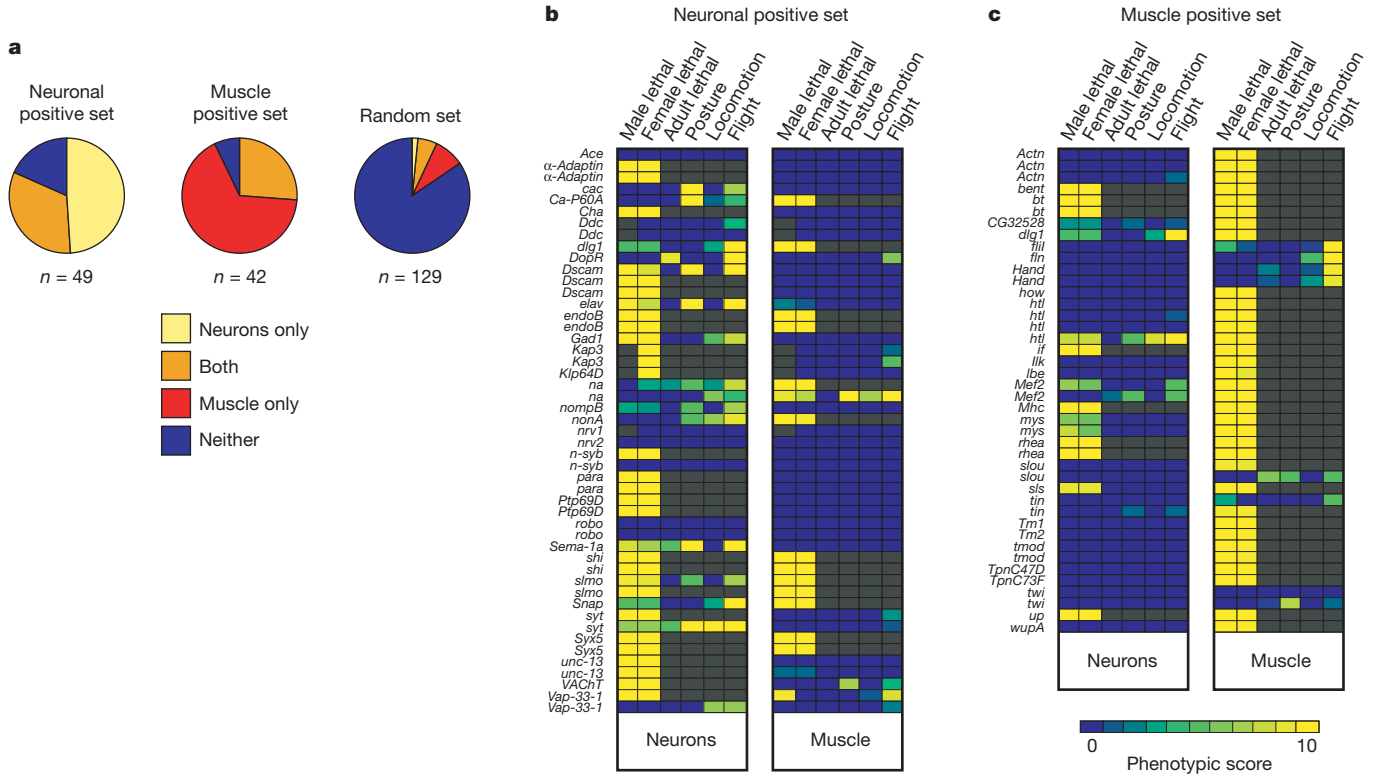

Figure 4 | RNAi in neurons and muscles. a, Percentages of neuronal and muscle positive-control lines, and randomly selected lines, that produce either a lethal, postural or behavioural phenotype when expressed with *elav-GAL4* (neurons) or *mef2-GAL4* (muscle). Note that, as anticipated, many of the neuronal positives also produced a phenotype with *mef2-GAL4* (33%), as did the muscle positives with *elav-GAL4* (26%); both sets are enriched but not exclusive for genes required in the respective tissue. **b**, **c**, Phenotypic data for 49 lines from the neuronal positive-control set (**b**) and 42 lines from the muscle positive-control set (**c**). Adult lethal indicates lethality by 7 days after eclosion. Data for posture and locomotion are collapsed from 2 and 5 different classes of defect, respectively, scored in the initial analysis. Flight scores indicate the fraction of flies falling immediately to the bottom when tapped into the top of a 1 m × 8 cm cylinder. All values are the average of two independent experiments.

METHODS SUMMARY

UAS-IR constructs. The pMF3 vector is derived from pUAST, but contains 10 rather than 5 tandem copies of the UAS element to enhance expression levels. On the basis of reports that introns enhance nuclear export[35], we included a short intron immediately 3′ to the inverted repeat. We did not include an intron within the inverted repeat itself, as is often done to improve its stability during cloning[36–38], because we did not have any difficulty cloning inverted repeats of less than 500 bp and did not observe any enhancement of RNAi efficiency with longer inverted repeats. PCR primers were designed using the Primer3 software[39].

Transgenic RNAi lines. Germline transformation was performed using a hyperactive P-element transposase[40]. For verification we extracted genomic DNA from single flies in 96-well plates and performed PCR with one gene-specific primer and a common primer in either the *hsp70* promoter region or the SV40 polyA region (Fig. 1a). Approximately 20% of lines failed the initial verification step; these lines were discarded and the construct re-injected. We believe these are mostly due to the loss of the inverted repeat during propagation in bacteria. To test whether the inverted repeat is stable in *Drosophila*, we verified a set of 192 lines that had been maintained for more than 2 yr (~35 generations) by amplifying both halves of the inverted repeat. In all of these lines, both halves of the inverted repeat were still present, and so we routinely verified transformants by amplifying only one half of the inverted repeat.

Test gene sets. Test genes for quantitative RT–PCR were chosen on the basis of available expression data[41,42]. We selected genes that were relatively highly expressed, reasoning that they should provide a robust measure of knock-down efficiency, which would, if anything, underestimate the average efficiency. Test sets for functional assays were chosen by manual curation from FlyBase and the literature. For all assays, transgenic RNAi males were crossed in duplicate to virgins carrying the relevant *GAL4* driver and, where appropriate, *UAS-Dcr-2*. Progeny were raised at 25 °C and scored blind to their genotype. Phenotypic categories in Figs 3 and 4 were partly derived by collapsing several distinct defects scored in the initial analysis. In all cases, there was very little phenotypic variation within the progeny of a single cross, with the exception of lethality (for which intermediate values indicate the fraction of animals surviving to the adult stage).

Full Methods and any associated references are available in the online version of the paper at www.nature.com/nature.

Received 28 February; accepted 22 May 2007.

1. Fire, A. *et al.* Potent and specific genetic interference by double-stranded RNA in *Caenorhabditis elegans*. *Nature* **391,** 806–811 (1998).
2. Boutros, M. *et al.* Genome-wide RNAi analysis of growth and viability in *Drosophila* cells. *Science* **303,** 832–835 (2004).
3. Berns, K. *et al.* A large-scale RNAi screen in human cells identifies new components of the p53 pathway. *Nature* **428,** 431–437 (2004).
4. Paddison, P. J. *et al.* A resource for large-scale RNA-interference-based screens in mammals. *Nature* **428,** 427–431 (2004).
5. Fraser, A. G. *et al.* Functional genomic analysis of *C. elegans* chromosome I by systematic RNA interference. *Nature* **408,** 325–330 (2000).
6. Gönczy, P. *et al.* Functional genomic analysis of cell division in *C. elegans* using RNAi of genes on chromosome III. *Nature* **408,** 331–336 (2000).
7. Kamath, R. S. *et al.* Systematic functional analysis of the *Caenorhabditis elegans* genome using RNAi. *Nature* **421,** 231–237 (2003).
8. Sönnichsen, B. *et al.* Full-genome RNAi profiling of early embryogenesis in *Caenorhabditis elegans*. *Nature* **434,** 462–469 (2005).
9. Reddien, P. W., Bermange, A. L., Murfitt, K. J., Jennings, J. R. & Sanchez Alvarado, A. Identification of genes needed for regeneration, stem cell function, and tissue homeostasis by systematic gene perturbation in planaria. *Dev. Cell* **8,** 635–649 (2005).
10. Newmark, P. A., Reddien, P. W., Cebria, F. & Sanchez Alvarado, A. Ingestion of bacterially expressed double-stranded RNA inhibits gene expression in planarians. *Proc. Natl Acad. Sci. USA* **100** (Suppl 1), 11861–11865 (2003).
11. Van Roessel, P., Hayward, N. M., Barros, C. S. & Brand, A. H. Two-color GFP imaging demonstrates cell-autonomy of GAL4-driven RNA interference in *Drosophila*. *Genesis* **34,** 170–173 (2002).
12. Roignant, J. Y. *et al.* Absence of transitive and systemic pathways allows cell-specific and isoform-specific RNAi in *Drosophila*. *RNA* **9,** 299–308 (2003).
13. Fortier, E. & Belote, J. M. Temperature-dependent gene silencing by an expressed inverted repeat in *Drosophila*. *Genesis* **26,** 240–244 (2000).
14. Kennerdell, J. R. & Carthew, R. W. Heritable gene silencing in *Drosophila* using double-stranded RNA. *Nature Biotechnol.* **18,** 896–898 (2000).

15. Lam, G. & Thummel, C. S. Inducible expression of double-stranded RNA directs specific genetic interference in *Drosophila*. *Curr. Biol.* **10,** 957–963 (2000).
16. Martinek, S. & Young, M. W. Specific genetic interference with behavioral rhythms in *Drosophila* by expression of inverted repeats. *Genetics* **156,** 1717–1725 (2000).
17. Brand, A. H. & Perrimon, N. Targeted gene expression as a means of altering cell fates and generating dominant phenotypes. *Development* **118,** 401–415 (1993).
18. Schuler, G. D. Sequence mapping by electronic PCR. *Genome Res.* **7,** 541–550 (1997).
19. Rubin, G. M. & Spradling, A. C. Genetic transformation of *Drosophila* with transposable element vectors. *Science* **218,** 348–353 (1982).
20. Ryder, E. *et al.* The DrosDel collection: a set of P-element insertions for generating custom chromosomal aberrations in *Drosophila melanogaster*. *Genetics* **167,** 797–813 (2004).
21. Kulkarni, M. M. *et al.* Evidence of off-target effects associated with long dsRNAs in *Drosophila melanogaster* cell-based assays. *Nature Methods* **3,** 833–838 (2006).
22. Ma, Y., Creanga, A., Lum, L. & Beachy, P. A. Prevalence of off-target effects in *Drosophila* RNA interference screens. *Nature* **443,** 359–363 (2006).
23. Duffy, J. B. GAL4 system in *Drosophila*: a fly geneticist's Swiss army knife. *Genesis* **34,** 1–15 (2002).
24. Bernstein, E., Caudy, A. A., Hammond, S. M. & Hannon, G. J. Role for a bidentate ribonuclease in the initiation step of RNA interference. *Nature* **409,** 363–366 (2001).
25. Lee, Y. S. *et al.* Distinct roles for *Drosophila* Dicer-1 and Dicer-2 in the siRNA/miRNA silencing pathways. *Cell* **117,** 69–81 (2004).
26. Williams, R. W. & Rubin, G. M. ARGONAUTE1 is required for efficient RNA interference in *Drosophila* embryos. *Proc. Natl Acad. Sci. USA* **99,** 6889–6894 (2002).
27. Hammond, S. M., Boettcher, S., Caudy, A. A., Kobayashi, R. & Hannon, G. J. Argonaute2, a link between genetic and biochemical analyses of RNAi. *Science* **293,** 1146–1150 (2001).
28. Liu, Q. *et al.* R2D2, a bridge between the initiation and effector steps of the *Drosophila* RNAi pathway. *Science* **301,** 1921–1925 (2003).
29. Caudy, A. A. *et al.* A micrococcal nuclease homologue in RNAi effector complexes. *Nature* **425,** 411–414 (2003).
30. Luo, L., Liao, Y. J., Jan, L. Y. & Jan, Y. N. Distinct morphogenetic functions of similar small GTPases: *Drosophila* Drac1 is involved in axonal outgrowth and myoblast fusion. *Genes Dev.* **8,** 1787–1802 (1994).
31. Ranganayakulu, G., Schulz, R. A. & Olson, E. N. Wingless signaling induces *nautilus* expression in the ventral mesoderm of the *Drosophila* embryo. *Dev. Biol.* **176,** 143–148 (1996).
32. Roman, G., Endo, K., Zong, L. & Davis, R. L. P{Switch}, a system for spatial and temporal control of gene expression in *Drosophila melanogaster*. *Proc. Natl Acad. Sci. USA* **98,** 12602–12607 (2001).
33. Stebbins, M. J. *et al.* Tetracycline-inducible systems for *Drosophila*. *Proc. Natl Acad. Sci. USA* **98,** 10775–10780 (2001).
34. McGuire, S. E., Le, P. T., Osborn, A. J., Matsumoto, K. & Davis, R. L. Spatiotemporal rescue of memory dysfunction in *Drosophila*. *Science* **302,** 1765–1768 (2003).
35. Maniatis, T. & Reed, R. An extensive network of coupling among gene expression machines. *Nature* **416,** 499–506 (2002).
36. Kalidas, S. & Smith, D. P. Novel genomic cDNA hybrids produce effective RNA interference in adult *Drosophila*. *Neuron* **33,** 177–184 (2002).
37. Lee, Y. S. & Carthew, R. W. Making a better RNAi vector for *Drosophila*: use of intron spacers. *Methods* **30,** 322–329 (2003).
38. Reichhart, J. M. *et al.* Splice-activated UAS hairpin vector gives complete RNAi knockout of single or double target transcripts in *Drosophila melanogaster*. *Genesis* **34,** 160–164 (2002).
39. Rozen, S. & Skaletsky, H. Primer3 on the WWW for general users and for biologist programmers. *Methods Mol. Biol.* **132,** 365–386 (2000).
40. Beall, E. L., Mahoney, M. B. & Rio, D. C. Identification and analysis of a hyperactive mutant form of *Drosophila* P-element transposase. *Genetics* **162,** 217–227 (2002).
41. Tomancak, P. *et al.* Systematic determination of patterns of gene expression during *Drosophila* embryogenesis. *Genome. Biol.* **3,** doi:10.1186/gb-2002-3-12-research0088 (2002).
42. Arbeitman, M. N. *et al.* Gene expression during the life cycle of *Drosophila melanogaster*. *Science* **297,** 2270–2275 (2002).

Supplementary Information is linked to the online version of the paper at www.nature.com/nature.

Acknowledgements We thank S. Bicker, J. Buch, M. Garstkiewicz, A. Gruber, D. Hofmann Rodrigues, K. Jäger, S. Krüttner, J. Mayerhofer, D. Muggenhumer, E. Muhr, K. Schernhuber, J. Schluder, A. Schmatz, C. Sturtzel, M. Vinzenz and W. Wolfgang for technical assistance, R. Lehmann for the original *hs-hid* lines, J. Mummery-Widmer, M. Yamazaki and J. Knoblich for suggesting the use of *pnr-GAL4*, R. Carthew for initial discussions on the effectiveness of *UAS-IR* transgenes, and B. Thompson and V. Siegel for helpful comments on the manuscript. F.S. was supported by a long-term postdoctoral fellowship from the Human Frontier Science Program. This work was supported by funds from the Austrian Academy of Sciences (IMBA) and Boehringer Ingelheim GmbH (IMP), and grants from the Austrian Science Fund and the European Union Framework Programme

Author Contributions G.D. established the methodology, and participated in and led the team that constructed the library. K.K. led this team during the finishing stages. D.C. and G.D. performed the bioinformatic analyses, G.D., F.S. and M.F. compiled all the data, which were analysed by G.D., B.J.D. and F.S. K.S. established the enhancing effect of *UAS-Dcr-2*. B.J.D. conceived and coordinated the project, and wrote the manuscript with input from G.D. and F.S. The remaining authors made major technical contributions to the construction of the library.

Author Information The transgenic RNAi library, including detailed information on each line, is available from the VDRC at ⟨http://www.vdrc.at⟩. Reprints and permissions information is available at www.nature.com/reprints. The authors declare no competing financial interests. Correspondence and requests for materials should be addressed to B.J.D. (dickson@imp.ac.at).

METHODS

Primer design. Primers were designed using the Primer3 software[39], generally selecting primers of 20–36 nucleotides, a melting temperature (T_m) of 66–70 °C, and a product size of 300–400 bp. These parameters were relaxed if no suitable primers were found. Usually, an *Eco*RI site was added to the left primer and an *Xba*I site to the right primer; if an endogenous recognition site for either enzyme occurred in the predicted product, *Bam*HI, *Bgl*II or *Mun*I was used as an alternative. e-PCR[43] was performed using a local version of Reverse e-PCR (version 2.3.0 for Windows). The template for e-PCR was either the Release 4.3 genome or transcriptome sequence, according to the template used for the actual PCR. For the transcriptome sequence, if the untranslated regions were unannotated, the protein coding sequence was used and extended by 50 bp of 5′ and 150 bp of 3′ genomic sequence. We allowed up to 2 mismatches and 2 gaps per primer, but not within the twelve 3′ nucleotides, and ±25 bp size variability compared to the expected product length.

Target predictions. Custom-designed Perl scripts were used to extract all possible 19-mers from all inverted repeat sequences and the Release 4.3 transcriptome, and to search for all perfect matches in either orientation. Target genes for each construct were ranked according to the total number of matches. The primary gene was defined as the top-ranked target (usually hit by 100% of 19-mers, but sometimes fewer owing to changes in the genome annotation). The number of hits on the second-ranked gene (if any) was used for the analysis in Fig. 1c. For calculation of s_{19} scores, on- and off-targets were defined using a cut-off of 80% of the number of matches on the primary target. A custom-designed Java script was used to determine the maximum number of contiguous CAN triplets.

Preparation of *UAS-IR* constructs. Target sequences were amplified by PCR from w^{1118} genomic DNA or mixed stage cDNA in 100 µl reactions. Fifty microlitres of the reaction was purified by gel filtration (SigmaSpin), digested with *Eco*RI, re-purified by gel filtration, ligated and digested with *Xba*I. The inverted repeats were then separated by gel electrophoresis, purified using NucleoSpin Multi-96 Extract kits (Macherey-Nagel), and ligated into pMF3. All cloning steps were performed manually in 96-well plates. Enzymes other than *Eco*RI and *Xba*I were used in some cases (see above). *Escherichia coli* SURE bacteria were transformed and plated in custom 48-well plates. Two colonies were grown from each transformation, and plasmid DNA extracted using QIAprep 96 Turbo Miniprep kits (Qiagen). The yield was typically 50 µl eluate with 150–200 ng µl^{-1} DNA per construct. Four microlitres of the extracted DNA was digested with *Xba*I and separated by gel electrophoresis to confirm the presence of the inverted repeat. For the positive clones with inserts of the predicted size, 10 µl of plasmid DNA was prepared for embryo injections by mixing with 3 µg of Δ2-3 transposase in a total volume of 12 µl.

Germline transformation. For each *UAS-IR* construct, ~40 dechorionated w^{1118} embryos were aligned on a 24 × 24 mm glass coverslip, dried for 20 min, covered with 10S Voltalef oil and microinjected using an Eppendorf FemtoJet with a micromanipulator mounted on a Zeiss Axiovert 200 inverted microscope. Borosilicate glass capillaries GC120TF-10 from Harvard Apparatus were pulled on a Suttner P-97 micropipette puller and opened on a Narishige EG-400 micropipette grinder. Injected embryos were placed in a moist chamber at 18 °C for 2 days, and then transferred to fly food vials supplemented with yeast paste and raised at 25 °C. Surviving adults were crossed out to w^{1118} flies, and transformants selected in the progeny using the w^+ marker. We typically obtained at least one transformant in 50–60% of each injection series. Initially, up to 4 lines were established per construct, but typically only up to 2 were retained after verification.

Verification and mapping. We extracted genomic DNA from single flies in 96-well plates. PCR reactions were set up with one specific primer (the right primer used to amplify the inverted repeat fragment) and one common primer (5′-GAGGCGCTTCGTCTACGGAGCGAC, located in the *hsp70* promoter region, or in some cases 5′-GCGCTCTAGACGTGTAGTAGACACTTTCGCTACGCAG, located in the SV40 polyA region; see Fig. 1a). Verified lines were then mapped to a specific chromosome by first crossing single transgenic males to virgins obtained from w^{1118}/Y, *hs-hid*; *Sp*/CyO and w^{1118}/Y, *hs-hid*; MKRS/TM2, y^+ stocks, and then crossing transgenic male CyO or MKRS progeny to w^{1118}; *Sp*, *hs-hid*/CyO and w^{1118}; *Ly*, *hs-hid*/TM3 *Sb* virgins, respectively. For the latter stocks, the original w^+ marker on each of the *hs-hid* transgenes had previously been removed by imprecise excision mediated by P-element transposase, so as to avoid any possible confusion between this w^+ marker and the w^+ marker on the *UAS-IR* transgene. Once the progeny of these crosses reached the 3rd instar stage, the parents were discarded and the vial heat shocked at 37 °C in a water bath for 1 h to kill progeny carrying the *hs-hid* chromosome. The surviving adults were then scored to determine which chromosome carried the *UAS-IR* transgene, and allowed to mate *inter se* to establish a balanced stock. Homozygous virgins and males were selected in subsequent generations to eliminate balancer chromosomes, where possible. For insertions on the X chromosome, *UAS-IR* males were crossed to *y w f*:= virgins obtained from a winscy, *hs-hid*/*y w f*:=/Y stock.

Quantitative RT–PCR. We designed PCR primers (19–23 nucleotides, T_m 60–63 °C) to amplify 150–350 bp fragments from the target transcripts that do not overlap with the original target regions of the *UAS-IR* constructs. Total RNA was extracted from twenty-five 2–4-day-old adult males using Trizol, yielding RNA at ~1.5 µg µl^{-1}. RNA (5 µg) was reverse transcribed using dN_6 random oligos and the SuperScript II Reverse Transcriptase kit (Invitrogen), yielding cDNA at ~1 µg µl^{-1}. Quantitative PCR reactions were then performed in 20 µl reactions using the SYBR Green JumpStart Taq ReadyMix kit (Sigma) and the Mastercycler realplex epgradientS system (Eppendorf) in 96-well optical plates (Eppendorf). For calibration experiments, PCRs for the test gene and α-tubulin (used as an internal standard) were run on a dilution series of 500, 50, 5 and 0 ng of wild-type cDNA template. After 40 cycles, dissociation analysis was performed to exclude from further experiments those primer pairs that produced primer dimers or amplified non-specific products. Standard curves were calculated for the test genes and α-tubulin[44], and experiments with correlation coefficients below 0.990 were excluded from further analysis. RNAi flies and controls were then assayed in duplicate by Real-Time PCR for the respective target gene and α-tubulin. The threshold cycle (C_t) values of the target gene were plotted on the wild-type standard curve to calculate target gene levels relative to wild type, and normalized for total cDNA input using α-tubulin levels. Relative knock-down levels of the two samples were averaged.

RNAi machinery transgenes. *UAS-Dcr-1*, *UAS-Dcr-2*, *UAS-AGO1*, *UAS-AGO2*, *UAS-tudor-SN*, and *UAS-R2D2* were prepared by amplifying the corresponding coding regions from genomic DNA and cloning them into the pUAST vector[17], verified by DNA sequencing, and injected into w^{1118} embryos for germline transformation[19]. We tested several insertions of each transgene in combination with RNAi transgenes against white (*w*) and sevenless (*sev*). For the experiments reported here, a *UAS-Dcr-2* transgene on the first chromosome was used. Similar enhancement effects were also observed with each of the three other *UAS-Dcr-2* transgene insertions tested.

Test sets. For the *Act5C-GAL4* assays, positive controls were selected by systematically extracting from FlyBase all loss-of-function mutant alleles reported to be associated with a lethal or visible phenotype. The final set of 473 genes was selected at random from an initial list of ~1,400 genes. The negative set was similarly selected from FlyBase, searching for genes with viable amorphic alleles with no reported phenotype, or in some cases a specific visible phenotype such as eye colour or body pigmentation. Positive controls for the *elav-GAL4* and *mef2-GAL4* assays were manually chosen by browsing FlyBase and the literature, selecting genes reported to function in neurons or muscles, though not necessarily exclusively in either. The random set used in these assays was an arbitrary subset of the random set used for the *Act5C-GAL4* assays.

Phenotypic analyses. For the ubiquitous, wing, eye and notum assays, lethal and morphological phenotypes were scored 3–4 d after eclosure. For the *elav-GAL4* and *mef2-GAL4* assays, viability was scored at eclosion and again at 5–7 d. Flies were aged in groups for 5–7 d before being scored for posture, locomotion, and flight. Males were used for autosomal *UAS-IR* insertions; females for insertions on the X chromosome. Flight assays were performed by dumping 20–30 males into a 1 m × 8 cm diameter plexiglass tube. Locomotion was assayed by tapping the flies to the bottom of the vial immediately before flight test, and estimating the fraction of flies that were slow or uncoordinated when climbing back up the wall of the vial. Wing posture was scored from the fraction of flies displaying an obvious held-out or erected wing phenotype. For all lethal, morphological and behavioural assays, crosses were scored blind to the genotype and duplicates were always run and scored in different batches on different days. Data presented in heat maps are the average of the two assays. For binary classifications, suitable threshold values were selected for each phenotypic parameter and a line was considered positive only if both assays exceeded the threshold.

43. Schuler, G. D. Sequence mapping by electronic PCR. *Genome Res.* **7**, 541–550 (1997).
44. Wong, M. L. & Medrano, J. F. Real-time PCR for mRNA quantitation. *Biotechniques* **39**, 75–85 (2005).